C.2

Copy 6
RM E55F20

NACA RM E55F20

NACA

RESEARCH MEMORANDUM

EFFECT OF INLET FLOW DISTORTION ON COMPRESSOR STALL AND ACCELERATION CHARACTERISTICS OF A J65-B-3 TURBOJET ENGINE

By David B. Fenn and Joseph N. Sivo

Lewis Flight Propulsion Laboratory
Cleveland, Ohio

NATIONAL ADVISORY COMMITTEE
FOR AERONAUTICS

WASHINGTON

November 18, 1955

NATIONAL ADVISORY COMMITTEE FOR AERONAUTICS

RESEARCH MEMORANDUM

EFFECT OF INLET FLOW DISTORTION ON COMPRESSOR STALL AND ACCELERATION CHARACTERISTICS OF A J65-B-3 TURBOJET ENGINE

By David B. Fenn and Joseph N. Sivo

SUMMARY

An investigation was conducted to determine the effects of inlet flow distortion on the compressor stall and engine acceleration characteristics of a J65-B-3 turbojet engine. A sinusoidal circumferential distortion and two abrupt radial tip flow distortions were introduced at the engine inlet at altitudes of 15,000, 35,000, and 50,000 feet and a flight Mach number of 0.8. All the inlet flow distortions investigated had total-pressure variations of about 20 percent of the area-weighted average inlet total pressure at rated corrected engine speed.

The circumferential distortion decreased the compressor-stall pressure ratio, the size of the fuel step required for stall, and the stall-limited maximum acceleration rate of the engine, primarily at high corrected engine speeds. The radial distortions decreased these parameters primarily at low corrected engine speeds near the knee in the stall line where the total-pressure variation of the distortion was only about 7 percent. This relatively small radial distortion increased the high-speed limit of rotating stall from 6200 to 6550 rpm and resulted in a 50-percent reduction in the stall-limited maximum acceleration rate at 6550 rpm. For fuel steps less than that required to stall the engine, the maximum acceleration rate obtained during a transient was found to be independent of the inlet flow distortions investigated.

INTRODUCTION

Nonuniform distributions of total pressure or air flow at the inlet of a turbojet engine can result from severe bends, shock-wave interaction, or excessively rapid diffusion in the inlet ducting. High-speed flight maneuvers where high angles of attack or yaw are encountered can also cause inlet pressure distortions. Such inlet pressure distortions caused by the inlet ducting and flight maneuvers have been

found to vary between 5 and 20 percent in both radial and circumferential directions. These distortions can impose large penalties in engine performance (ref. 1) and may result in compressor stall, combustor blowout, or even structural failure of the engine (ref. 2).

As part of a general program at the NACA Lewis laboratory, the effects of radial and circumferential inlet pressure distortions on the stall and acceleration characteristics of a J65-B-3 turbojet engine were determined in an altitude test chamber. Two radial distortions with the low-pressure region at the tip section of the compressor and one sinusoidal circumferential distortion were introduced into the engine by blocking portions of the inlet duct with fine-mesh wire screens. Data were obtained with the rated exhaust nozzle at simulated altitudes of 15,000, 35,000, and 50,000 feet and a flight Mach number of 0.8 over a range of corrected engine speeds from 5000 to 9000 rpm. The compressor pressure ratio at stall, the maximum acceleration rate of the engine during fuel-flow transients, and the step increase of fuel flow required to stall the compressor were determined with each configuration.

APPARATUS

Engine

The J65-B-3 turbojet engine used in this investigation (fig. 1) has a 13-stage axial-flow compressor, an annular prevaporizing-type combustor, and a two-stage turbine. The engine was equipped with a fixed exhaust nozzle sized to give rated exhaust gas temperature (1166° F) at rated engine speed (8300 rpm) at sea-level static conditions. The rated engine air flow at these conditions is 118 pounds per second. The fuel used throughout this investigation was MIL-F-5624A grade JP-4.

Installation

The engine was installed in an altitude test chamber as shown in figure 1. A bulkhead with a labyrinth seal around the front of the engine was used to allow independent control of the inlet and exhaust pressures. The laboratory air systems were used to supply air to the engine and to remove the exhaust gases. An automatic rapid-response valve was mounted in the front bulkhead to maintain constant inlet total pressure during engine accelerations. An electronically controlled rapid-response fuel valve (ref. 3) was used to approximate step changes in engine fuel flow.

Inlet Distortion Screens

Inlet flow distortions were introduced into the engine by blocking portions of inlet duct with fine-mesh wire screens as shown in figure 2. A 1/4-inch mesh screen covered the entire inlet annulus 39 inches ahead of the inlet guide vanes for both the undistorted and distorted configurations and supported the fine-mesh distortion screens. For the radial distortions the fine-mesh screens were placed so that a low-pressure region existed at the blade tip section of the compressor inlet. Two radial distortions were investigated: one with the low-pressure region covering approximately 30 percent of the passage height at the inlet guide vanes and the other covering 50 percent. These two configurations are referred to as "30-percent-blockage radial" and "50-percent-blockage radial" distortions in this report. To prevent the radial distortions from "washing out" between the screen and the compressor inlet, a splitter duct that was concentric with the engine centerline was used. For the circumferential distortion eight screen segments were placed as shown in figure 2(b) to give a gradual variation of total pressure around the compressor inlet.

Instrumentation

The location and amount of instrumentation used during this investigation are shown in figure 3. Steady-state pressures were measured with manometers and were photographically recorded. Self-balancing potentiometers were used to measure temperatures, and steady-state fuel flow was measured with calibrated rotameters. Changes in total pressure during engine transients were measured with calibrated aneroid-type pressure transducers having strain-gage elements. Fuel-flow changes were measured with calibrated vane-type flow meters, and engine speed was measured with a magnetic pulse generator. A six-channel strip-chart recorder was used to record the output of all transient instrumentation. The chart speed used for most of the transients was 25 millimeters per second. The frequency response of the transient pressure instrumentation was on the order of 20 cps. However, these instruments would respond to frequencies of 75 cps with some reduction in amplitude. All transient instrumentation was calibrated against steady-state instrumentation.

PROCEDURE

The flight conditions selected for this investigation are presented for each configuration in the following table:

Distortion	Altitude, ft		
	[a]15,000	[b]35,000	[b]50,000
None	√	√	√
30-Percent-blockage radial	√	√	√
50-Percent-blockage radial		√	
Circumferential		√	

[a]Inlet temperature varied from 70° to 85° F.

[b]NACA standard temperature.

3750

All configurations were operated at NACA standard pressure at a simulated flight Mach number of 0.8 assuming 100-percent total-pressure recovery in the portion of the inlet duct having only the 1/4-inch mesh screen. At each flight condition the engine was operated with the fixed exhaust nozzle over a range of corrected engine speeds from 5000 rpm to the maximum allowable. The speed range was divided into 500-rpm increments, and at each base speed successively larger step increases in fuel flow were made until compressor stall was encountered. The engine was allowed to accelerate only about 1000 rpm for each fuel step because of either high turbine-outlet temperature or manometer-board limitations. However, the maximum acceleration rate following a fuel step occurs within the first few hundred rpm of the acceleration (see ref. 4), and this point was selected for comparison of the configurations investigated. The acceleration rate of the engine was determined from the slope of the engine-speed trace. The symbols used throughout this report are defined in the appendix.

RESULTS AND DISCUSSION

Definition of Inlet Flow Distortions

The total- and static-pressure profiles of the circumferential distortion obtained with the engine operating at rated corrected speed at an altitude of 35,000 feet and a flight Mach number of 0.8 are presented in figure 4. The circumferential distortion consisted of a stepwise variation in total pressure around the duct (fig. 4(a)). The magnitude of the total-pressure variation was about 19 percent of the area-weighted average inlet total pressure. These profiles were measured at station 2, which was $19\frac{5}{8}$ inches ahead of the inlet guide vanes and approximately halfway between the screens and the guide vanes. This circumferential distortion caused a variation in compressor-inlet velocity from 525 feet per second in the unblocked portion of the duct to 260 feet per second behind the maximum blockage. Because of this velocity difference and the static-pressure gradient measured at station 2

(fig. 4(b)), the circumferential distortion was probably attenuated to some extent between station 2 and the inlet guide vanes.

The total- and static-pressure profiles of the 30-percent-blockage radial distortion measured with the engine operating at rated corrected engine speed at an altitude of 35,000 feet and a flight Mach number of 0.8 are shown in figure 5. Because a radial distortion has been found to wash out much more rapidly than a circumferential distortion, a splitter duct was installed to separate the blocked and unblocked portions of the inlet duct. The splitter duct extended from the screens to the inlet guide vanes where traversing total- and static-pressure probes were located. Figure 5(a) shows that the 30-percent-blockage radial distortion was characterized by a 21-percent $\left(\frac{P_{max} - P_{min}}{P_{av}}\right)$ abrupt change in total pressure, with the low-pressure region at the tip section covering about 30 percent of the inlet-guide-vane length. Use of the splitter duct to maintain the total-pressure distortion resulted in a static-pressure distortion of about 10 percent at rated engine speed (fig. 5(b)). The compressor-inlet velocity with the 30-percent-blockage radial distortion varied from 325 feet per second in the blocked portion of the inlet duct to 550 feet per second in the unblocked portion. The pressure profiles of the 50-percent-blockage radial distortion were similar to those for the 30-percent-blockage radial distortion except that the low-pressure region covered a larger portion of the inlet duct. Therefore, the pressure profiles of the 50-percent-blockage radial distortion are not shown.

Because the pressure loss through a screen is a function of corrected air flow, the magnitude of the distortion imposed on the engine by each screen configuration varies with corrected engine speed. The variation of percent distortion $\left(\frac{P_{max} - P_{min}}{P_{av}}\right)$ with corrected engine speed for the circumferential and radial distortions is presented in figure 6. In all cases, an increase in corrected engine speed from 6000 to 8300 rpm resulted in an increase in percent distortion from about 5 to 20 percent.

Acceleration Limits

The acceleration rate of a turbojet engine is generally limited by compressor stall or excessive turbine-inlet temperature. Only the compressor stall limit will be considered herein. Some typical records obtained during transients following step increases in fuel flow are presented in figure 7 where time histories of compressor-inlet and -outlet total pressures, fuel flow, and engine speed are shown. Because

of the inherent lag in the transient fuel-flow instrumentation, it is believed that the fuel flow more closely approximated a step increase than these records indicate. An acceleration free of stall is shown in figure 7(a). After the fuel step was initiated, engine speed and compressor-outlet total pressure rose smoothly until fuel flow was cut back to the steady-state value. With sufficiently large fuel steps the compressor pressure ratio rises far enough above the steady-state operating line to cause the compressor to stall. An example of such a transient is presented in figure 7(b), in which the compressor-outlet pressure increased during the initial portion of the transient to the stall point defined by the first sharp drop in compressor-outlet pressure. In this example (fig. 7(b)) the stall point was followed by a surging condition in the engine characterized by a high-amplitude, low-frequency pulsation (8 to 10 cps) of compressor-outlet total pressure. Superimposed on the engine surge is a higher frequency pulsation, probably caused by rotating stall in the compressor. With this engine, the stall point may be followed by compressor stall without engine surge. Compressor stall without engine surge following the stall point (fig. 7(c)) is characterized by a lower amplitude and higher frequency (40 to 50 cps) pulsation of compressor-outlet total pressure. Compressor stall of this type is probably a single-zone rotating stall.

With uniform inlet flow the stall point was always followed by engine surge for corrected engine speeds above 6000 rpm at an altitude of 35,000 feet and a flight Mach number of 0.8. Below 6000 rpm the stall point could be followed by either compressor stall or engine surge. With the inlet flow distortions investigated, the speed range in which engine surge followed the stall point was restricted to higher corrected engine speeds. With circumferential distortion engine surge was encountered above 6500 rpm, and with the 30-percent-blockage radial distortion surge was only encountered above 7800 rpm. Because both compressor stall and engine surge are initiated by compressor blade stall (stall point), the acceleration limit will be referred to as "stall" in this report.

Compressor Pressure Ratio at Stall

The compressor pressure ratio at stall obtained with uniform inlet flow is presented as a function of corrected engine speed in figure 8 for the three flight conditions included in this investigation. The steady-state operating line for each flight condition is also shown.

A discontinuity (or knee) in the stall line exists at low corrected engine speeds. An extension of the upper portion of the stall line from the knee to the steady-state operating line closely approximates the high-speed limit of rotating stall. Rotating stall of from one to five zones has been found to exist in this compressor at low corrected engine

speeds (ref. 5). The high-speed limit of rotating stall is indicated by the shaded area on figure 8 for an altitude of 35,000 feet. Figure 8 also shows that increasing the altitude from 15,000 to 50,000 feet resulted in a decrease in the compressor-stall pressure ratio and in an increase of about 400 rpm in the corrected engine speed at which the knee in the stall line occurred. Because of fuel-pump limitations, the stall limit was not determined at an altitude of 15,000 feet for engine speeds above the knee in the stall line.

Effect of circumferential distortion. - The effect of circumferential inlet pressure distortion on the compressor pressure ratio for stall is presented in figure 9 for an altitude of 35,000 feet and a flight Mach number of 0.8. The compressor pressure ratio at stall based on average pressures (fig. 9(a)) was lowered by the circumferential distortion, although neither the corrected engine speed at the stall-line knee nor the steady-state operating line was affected.

With circumferential distortion, axial-flow compressors have been found to stall when any circumferential segment of the compressor reaches the normal stall pressure ratio (ref. 2). This is illustrated in figure 9(b), where the maximum local pressure ratio at stall is compared with the stall pressure ratio obtained without distortion. The maximum local pressure ratio was calculated from minimum compressor-inlet and -outlet total pressures. The minimum compressor-outlet total pressure was only about 2 percent lower than the average and occurred in the same axial segment as the minimum compressor-inlet total pressure.

Effect of radial distortion. - The 30-percent-blockage radial distortion decreased the average compressor pressure ratio for stall at both 35,000 and 50,000 feet as shown by figures 10(a) and (b), respectively. In addition, for each flight condition the corrected engine speed at which the knee in the stall line occurred was increased approximately 350 rpm above the engine speed at which it occurred with uniform inlet flow. The magnitude of distortion $\left(\frac{P_{max} - P_{min}}{P_{av}}\right)$ that caused this shift was only 7 percent (see fig. 6(b)). This shift in corrected engine speed at the stall-line knee can be explained from compressor theory. Generally, when a compressor is operating in the low-speed range, the air flow through the compressor is limited by choking in the rear stages; the choking condition forces the inlet stages to operate at stalling angles of attack. As engine speed is increased, the choking condition in the rear stages of the compressor is relieved because of the increased air density at the rear stages, thus decreasing the angle of attack of the inlet stages until at some speed the blades unstall. The low-speed stall condition of the inlet stages was characterized by rotating stall which occurred at the blade tips. The reduction of air flow in this region by the radial distortion

caused the stall condition to persist to a higher engine speed than with uniform inlet flow and hence caused the knee in the stall line to occur at a higher engine speed.

A comparison of the compressor-stall pressure-ratio lines obtained with the 30-percent- and 50-percent-blockage radial distortions is presented in figure 10(c). Because the two radial distortions investigated had essentially the same effect on the stall pressure ratio, the remainder of the discussion will deal primarily with the circumferential and 30-percent-blockage radial inlet flow distortions.

Fuel Flow for Stall

Uniform inlet flow. - The maximum fuel step which the engine could be subjected to without encountering compressor stall is of interest from a control point of view and is presented in figure 11 for uniform inlet flow. The relation between final fuel flow and initial corrected engine speed is shown, together with the steady-state operating lines for a flight Mach number of 0.8. It can be seen that the steady-state fuel flow could be more than doubled in a step change without causing compressor stall at any of the engine speeds or flight conditions investigated. An increase in altitude from 35,000 to 50,000 feet resulted in a decrease in stall-limit fuel flow and an increase in the speed for the stall-line knee.

Effect of inlet flow distortion. - The effect of the circumferential and the 30-percent-blockage radial distortions on the fuel step for stall is presented in figure 12 for an altitude of 35,000 feet and a flight Mach number of 0.8. The circumferential distortion (fig. 12(a)) had no effect on corrected stall-limit fuel flow at low speeds, but at high corrected speeds it reduced the fuel flow about 13 percent from that observed with uniform inlet flow. The 30-percent-blockage radial distortion (fig. 12(b)) decreased the corrected stall-limit fuel flow in the engine speed range between 6100 and 7200 rpm as a result of the shift in the stall-line knee but had no apparent effect at high corrected engine speeds. The corrected stall-limit fuel flow was the same, within experimental scatter, for the two radial distortions investigated.

Maximum Acceleration Rate

Uniform inlet flow. - The maximum acceleration rate of the engine occurred about 100 rpm after the fuel step was initiated and was calculated from the slope of the engine-speed trace. The accuracy of this method of determining acceleration rate is of the order of ±10 percent. A plot of corrected maximum acceleration rate as a function of corrected engine speed is presented in figure 13 for the uniform-inlet-flow configuration at an altitude of 35,000 feet and a flight Mach number of

0.8. The stall-limited acceleration line represents the highest maximum acceleration rate obtained with stall-free fuel steps. Lines of constant corrected fuel-step size were cross-plotted onto this figure from plots of corrected maximum acceleration rate against corrected fuel-step size for several corrected engine speeds. A maximum corrected acceleration rate of 2500 rpm per second was obtained at a corrected engine speed of 7400 rpm.

3750

Effect of inlet flow distortion. - The effect of the circumferential and 30-percent-blockage-radial distortions on the stall-limited maximum acceleration rate is presented in figure 14 for an altitude of 35,000 feet and a flight Mach number of 0.8. The effect of the distortions on stall-limited maximum acceleration rate is similar to the effect of distortion on stall-limited fuel flow. The circumferential distortion decreased stall-limited maximum acceleration rate at high corrected engine speeds, whereas the greatest effect of the 30-percent-blockage radial distortion occurred at corrected speeds near the knee in the stall line. At the stall-line knee (6550 rpm) the total-pressure variation of this radial distortion was only about 7 percent, but the stall-limited maximum acceleration rate of the engine was reduced by about 50 percent.

2-S2

For stall-free fuel steps the corrected maximum acceleration rate of a turbojet engine can be correlated with the fuel-step parameter $\Delta W_f/N\delta$ derived in reference 4. The variation of corrected maximum acceleration rate with the fuel-step parameter is presented in figure 15 for the uniform inlet flow, the 30-percent-blockage radial, and the circumferential configurations at an altitude of 35,000 feet and a flight Mach number of 0.8. The data for the three configurations fall within a ±12-percent scatter band. Because the probable accuracy of the measured acceleration rate is only about ±10 percent, no effect of inlet flow distortion on the stall-free maximum acceleration rate could be detected.

SUMMARY OF RESULTS

A sinusoidal circumferential inlet flow distortion and two radial tip flow distortions were introduced at the inlet of a J65-B-3 turbojet engine. All the inlet flow distortions investigated had variations of inlet total pressure of about 20 percent at rated corrected engine speed.

The circumferential distortion decreased the compressor-stall pressure ratio, the size of the fuel-flow step required for stall, and the stall-limited maximum acceleration rate, primarily at high corrected engine speeds. The radial distortions decreased these

[redacted]

parameters primarily in the corrected speed range where the knee in the stall line occurred. In this speed range the inlet radial pressure distortion was about 7 percent. This relatively small radial distortion increased the high-speed limit of rotating stall from 6200 to 6550 rpm and resulted in a 50-percent reduction in the stall-limited maximum acceleration rate of the engine at 6550 rpm.

For fuel steps less than that required to stall the engine, the maximum acceleration rate obtained during a transient was found to be independent of the inlet flow distortions investigated.

Lewis Flight Propulsion Laboratory
National Advisory Committee for Aeronautics
Cleveland, Ohio, June 23, 1955

[redacted]

APPENDIX - SYMBOLS

The following symbols are used in this report:

N engine speed, rpm

N' maximum acceleration rate of engine following step increase in fuel flow, rpm/sec

P total pressure, lb/sq ft abs

p static pressure, lb/sq ft abs

W_f fuel flow, lb/hr

ΔW_f change in fuel flow during transient, lb/hr

δ area-weighted average inlet total pressure divided by NACA standard sea-level pressure

θ inlet total temperature divided by NACA standard sea-level temperature

Subscripts:

2 measuring station $19\frac{5}{8}$ in. ahead of inlet guide vanes

3 compressor outlet

av area-weighted average

max maximum

min minimum

REFERENCES

1. Huntley, S. C., Sivo, Joseph N., and Walker, Curtis L.: Effect of Circumferential Total-Pressure Gradients Typical of Single-Inlet Duct Installations on Performance of an Axial-Flow Turbojet Engine. NACA RM E54K26a, 1955.

2. Walker, Curtis L., Sivo, Joseph N., and Jansen, Emmert T.: Effect of Unequal Air-Flow Distribution from Twin Inlet Ducts on Performance of an Axial-Flow Turbojet Engine. NACA RM E54E13, 1954.

3. Otto, Edward W., Gold, Harold, and Hiller, Kirby W.: Design and Performance of Throttle-Type Fuel Controls for Engine Dynamic Studies. NACA TN 3445, 1955.

4. Dobson, W. F., and Wallner, Lewis E.: Acceleration Characteristics of a Turbojet Engine with Variable-Position Inlet Guide Vanes. NACA RM E54I30, 1955.

5. Calvert, Howard F., Braithwaite, Willis M., and Mederios, Arthur: Rotating-Stall and Rotor-Blade-Vibration Survey of a 13-Stage Axial-Flow Compressor in a Turbojet Engine. NACA RM E54J18, 1955.

[redacted]

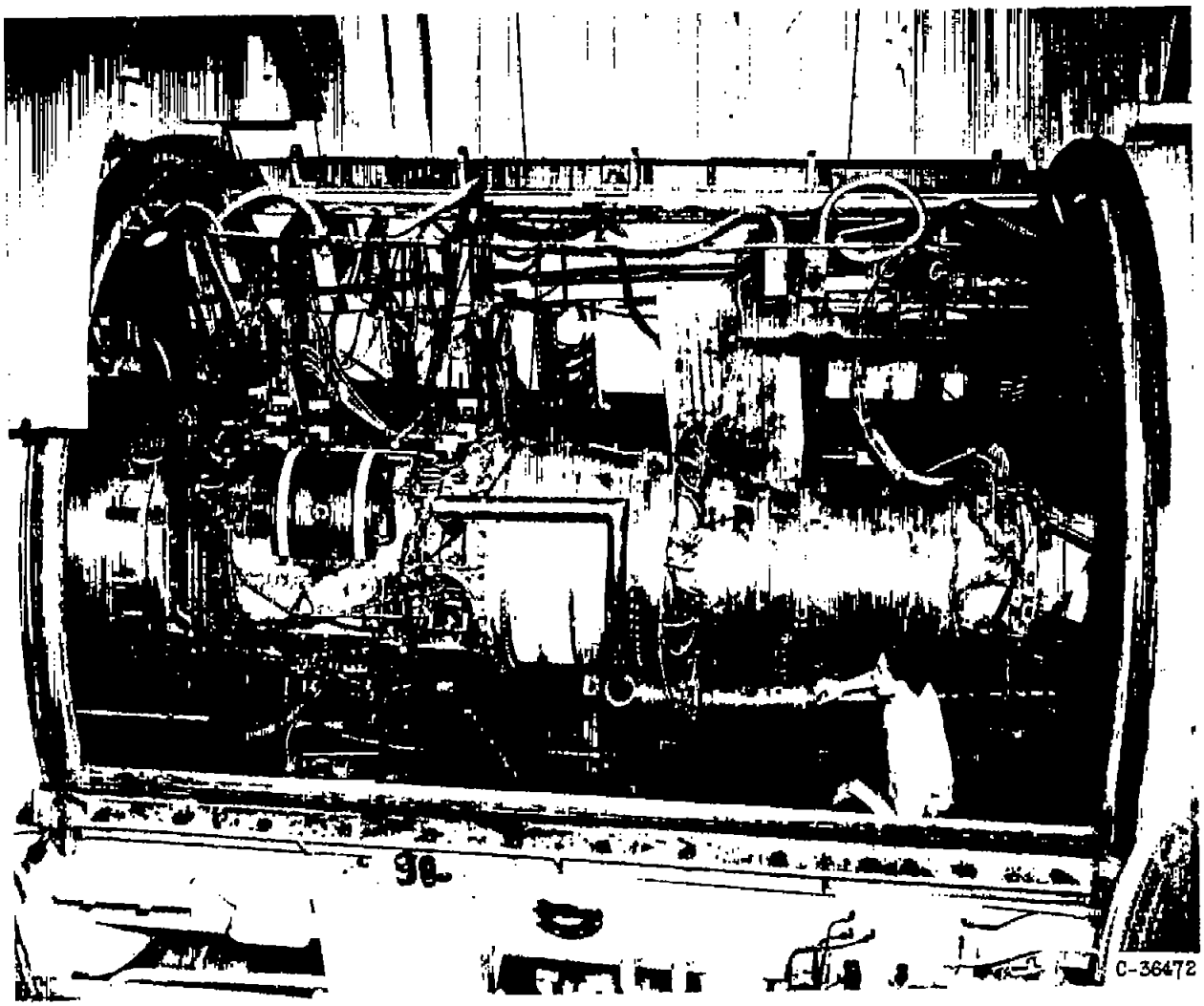

Figure 1. - Engine installation.

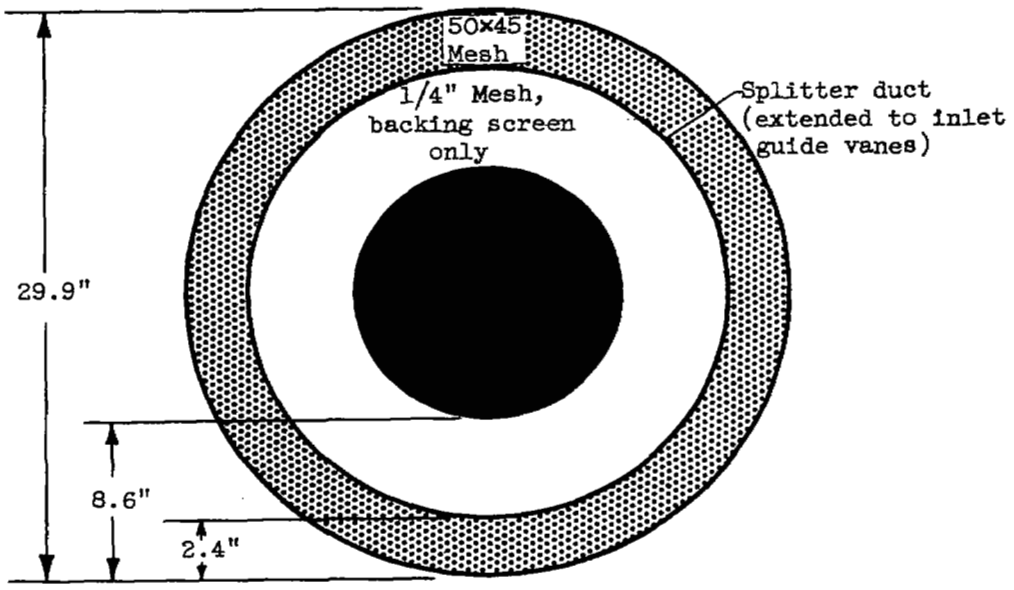

(a) 30-Percent-blockage radial distortion.

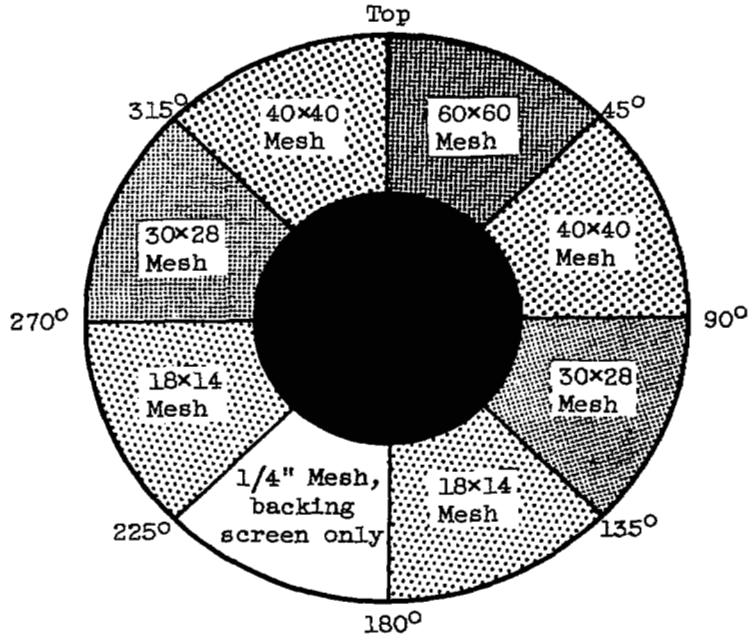

(b) Circumferential distortion.

Figure 2. - Screen placement for inlet air distortions (viewed downstream).

[redacted]

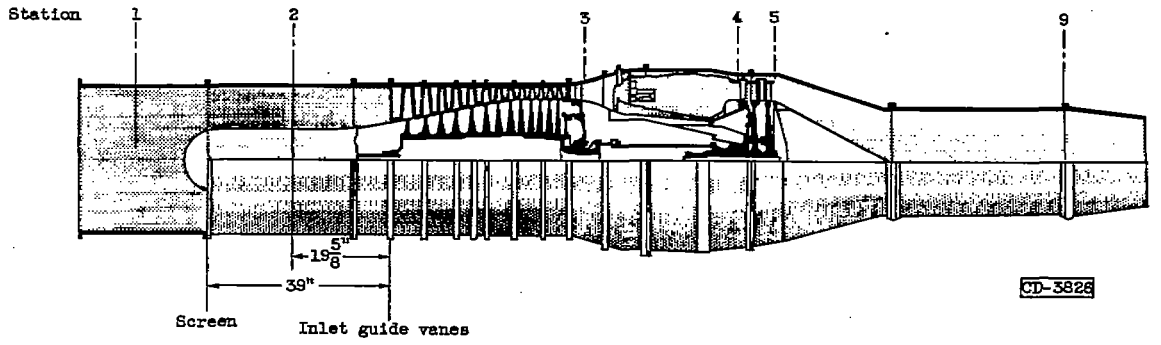

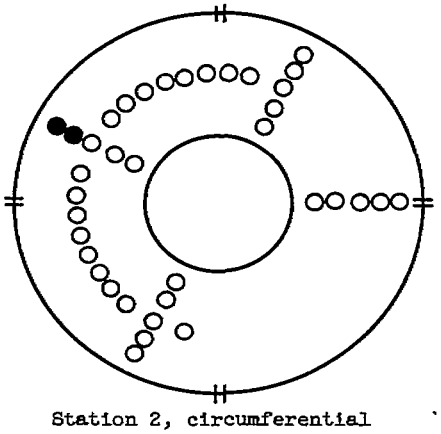

Station 2, circumferential distortion

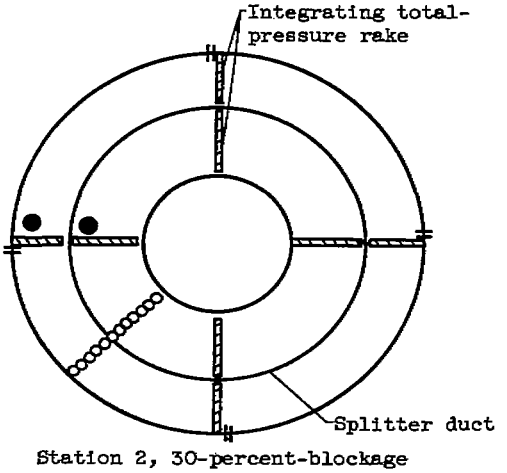

Station 2, 30-percent-blockage radial distortion

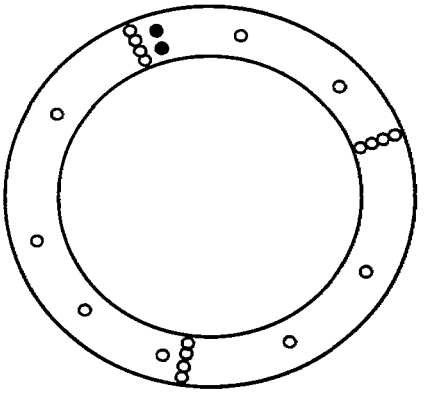

Station 3

o Total pressure
= Static pressure (wall)
● Transient total pressure

Figure 3. - Instrumentation. (All instrumentation sketches viewed downstream; no scale.)

[redacted]

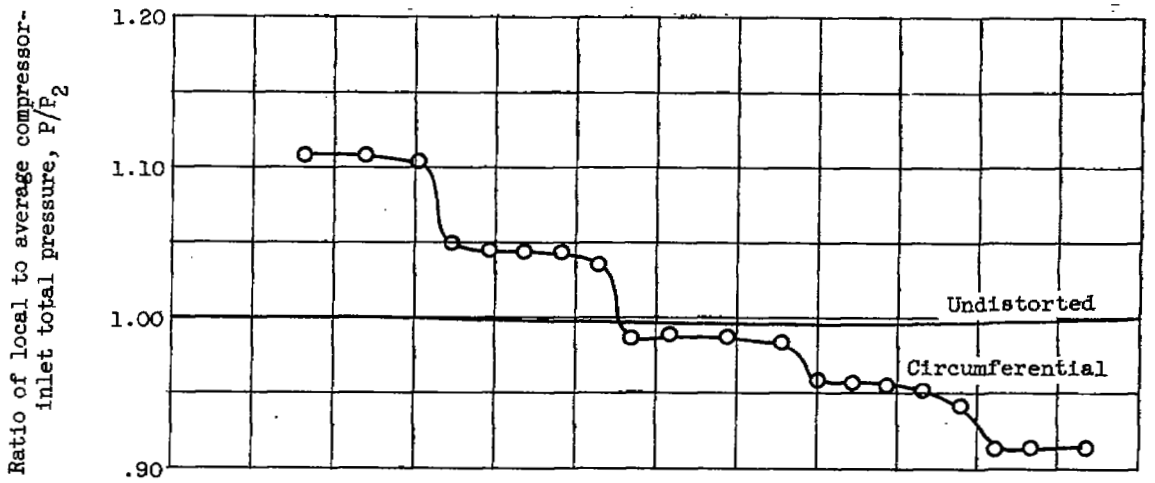

(a) Total-pressure station 2.

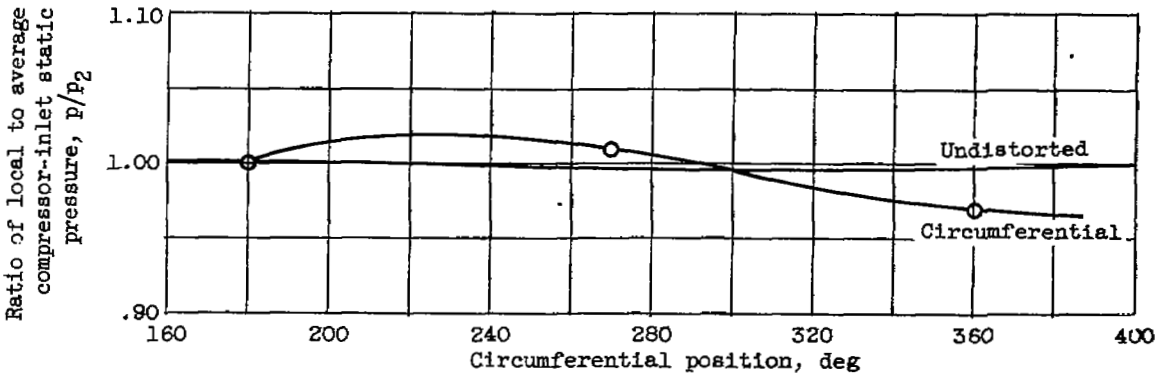

(b) Static-pressure station 2.

Figure 4. - Pressure profiles for circumferential inlet flow distortion. Altitude, 35,000 feet; flight Mach number, 0.8; corrected engine speed, 8300 rpm.

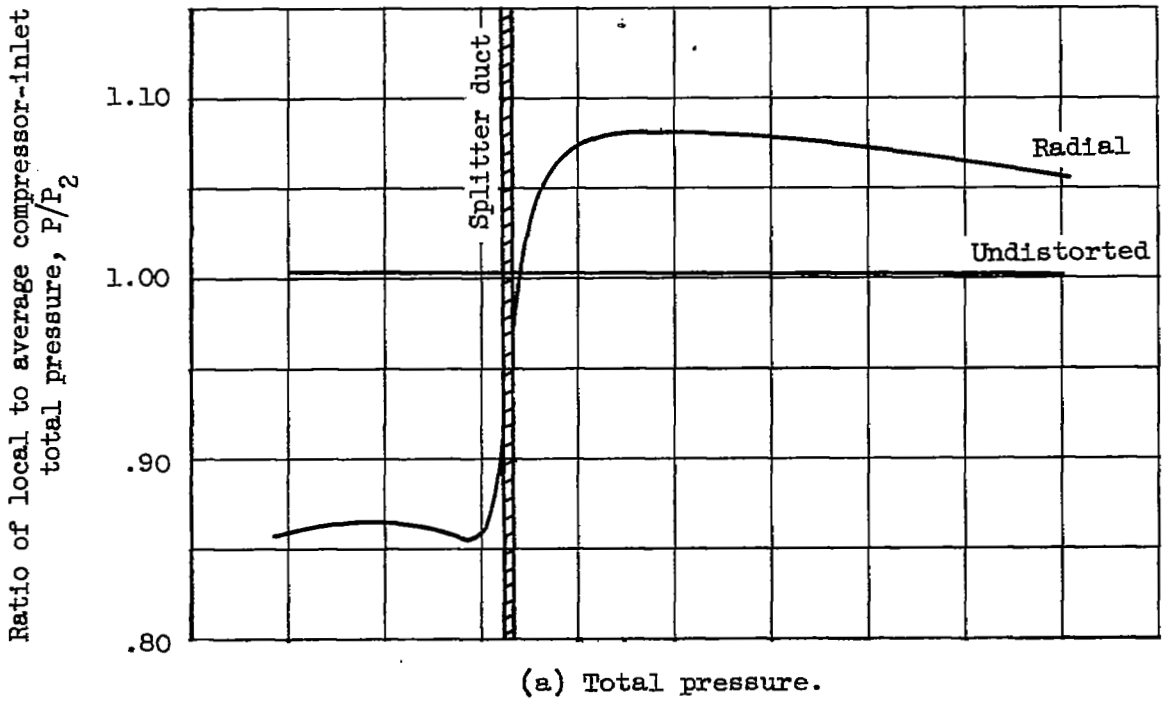

(a) Total pressure.

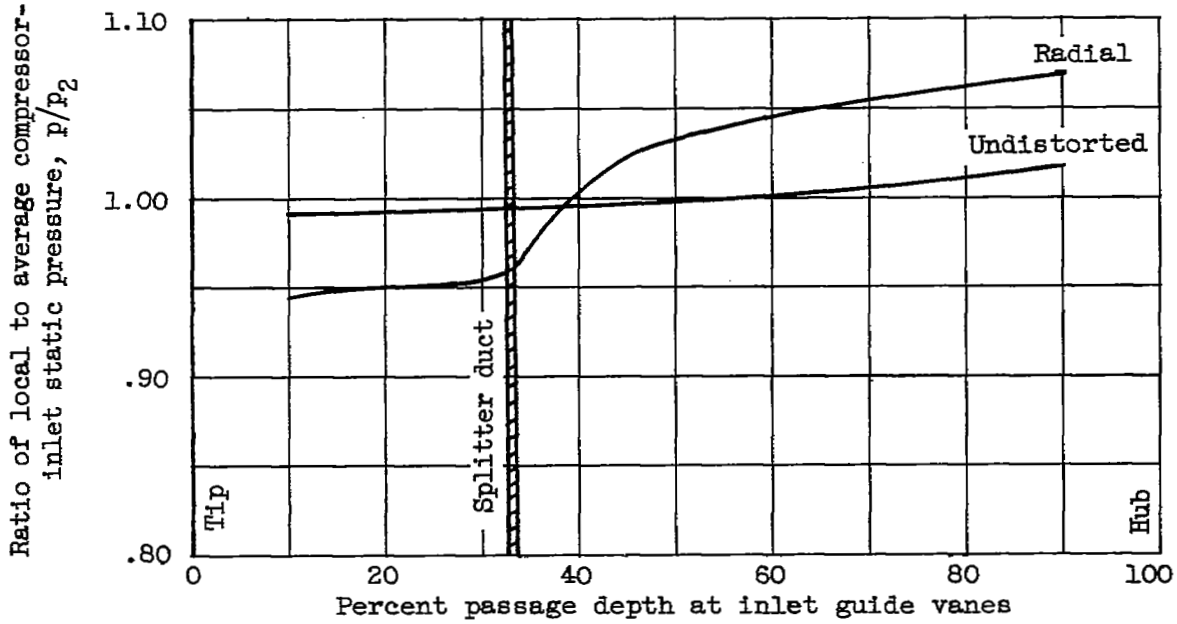

(b) Static pressure.

Figure 5. - Pressure profiles for 30-percent-blockage radial distortion. Inlet-guide-vane survey; altitude, 35,000 feet; flight Mach number, 0.8; corrected engine speed, 8300 rpm.

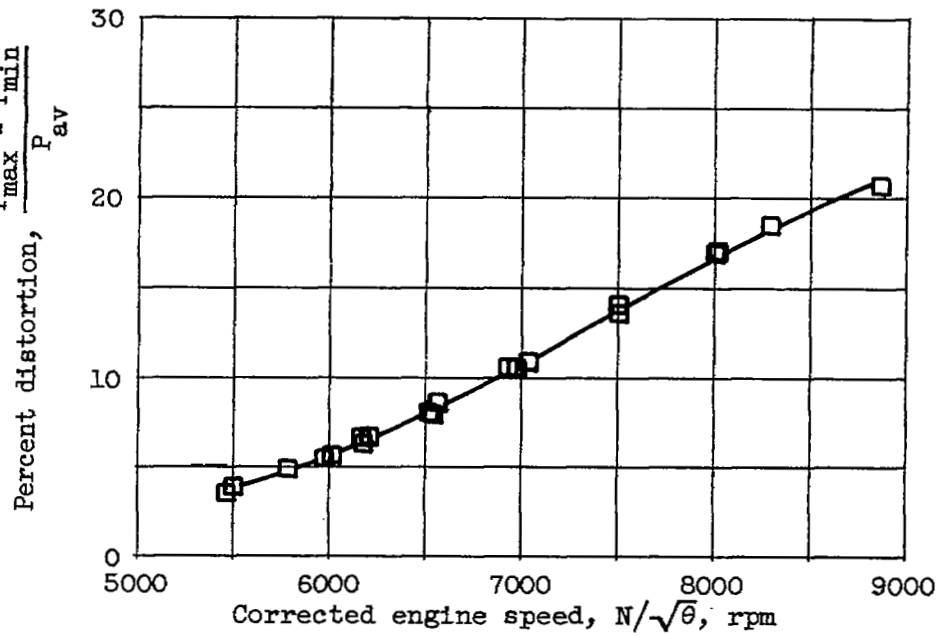

(a) Circumferential distortion; altitude, 35,000 feet.

Figure 6. - Variation of percent inlet total-pressure distortion with corrected engine speed. Flight Mach number, 0.8.

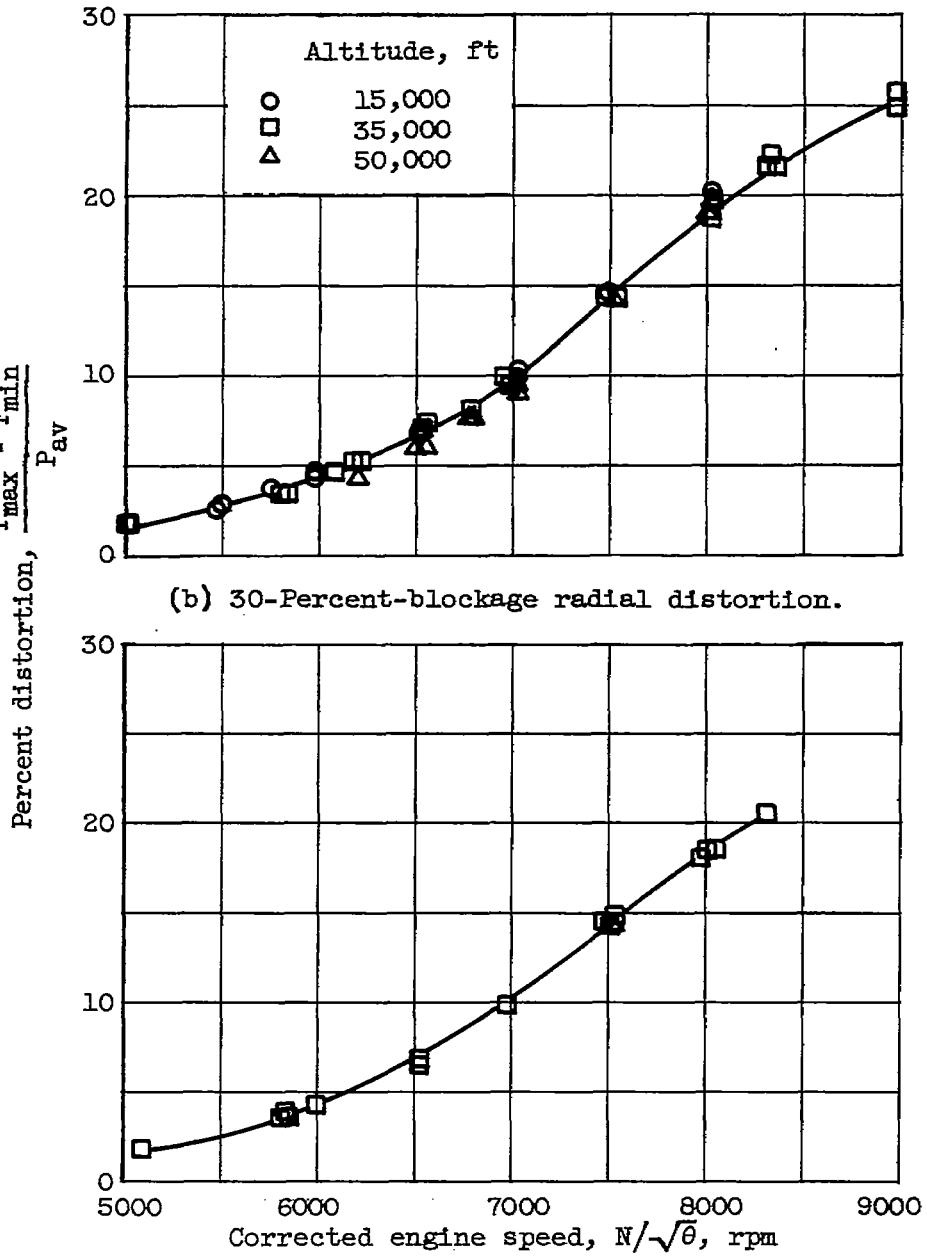

(b) 30-Percent-blockage radial distortion.

(c) 50-Percent-blockage radial distortion; altitude, 35,000 feet.

Figure 6. - Concluded. Variation of percent inlet total-pressure distortion with corrected engine speed. Flight Mach number, 0.8.

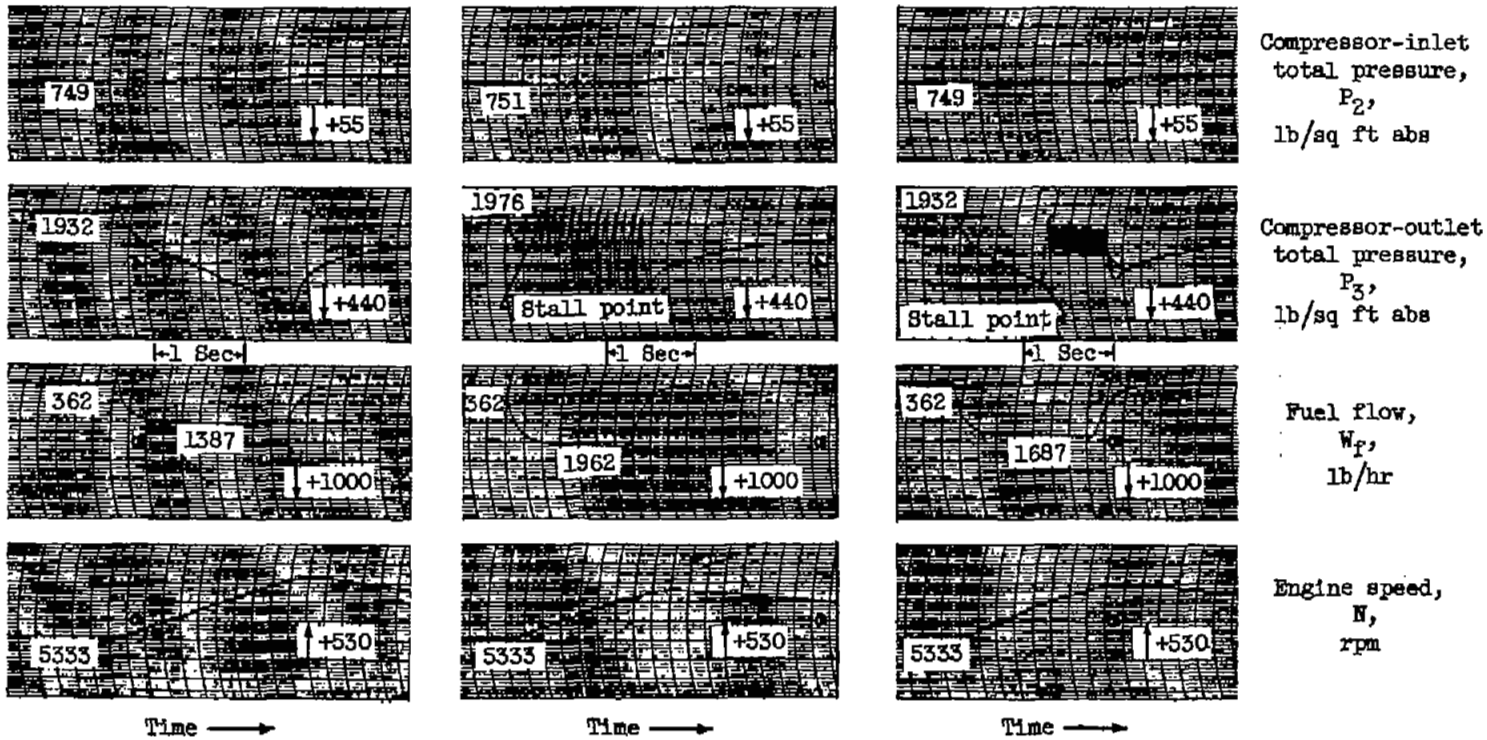

(a) Acceleration free of compressor stall.

(b) Acceleration into compressor stall with engine surge.

(c) Acceleration into compressor stall without engine surge.

Figure 7. - Typical transient traces.

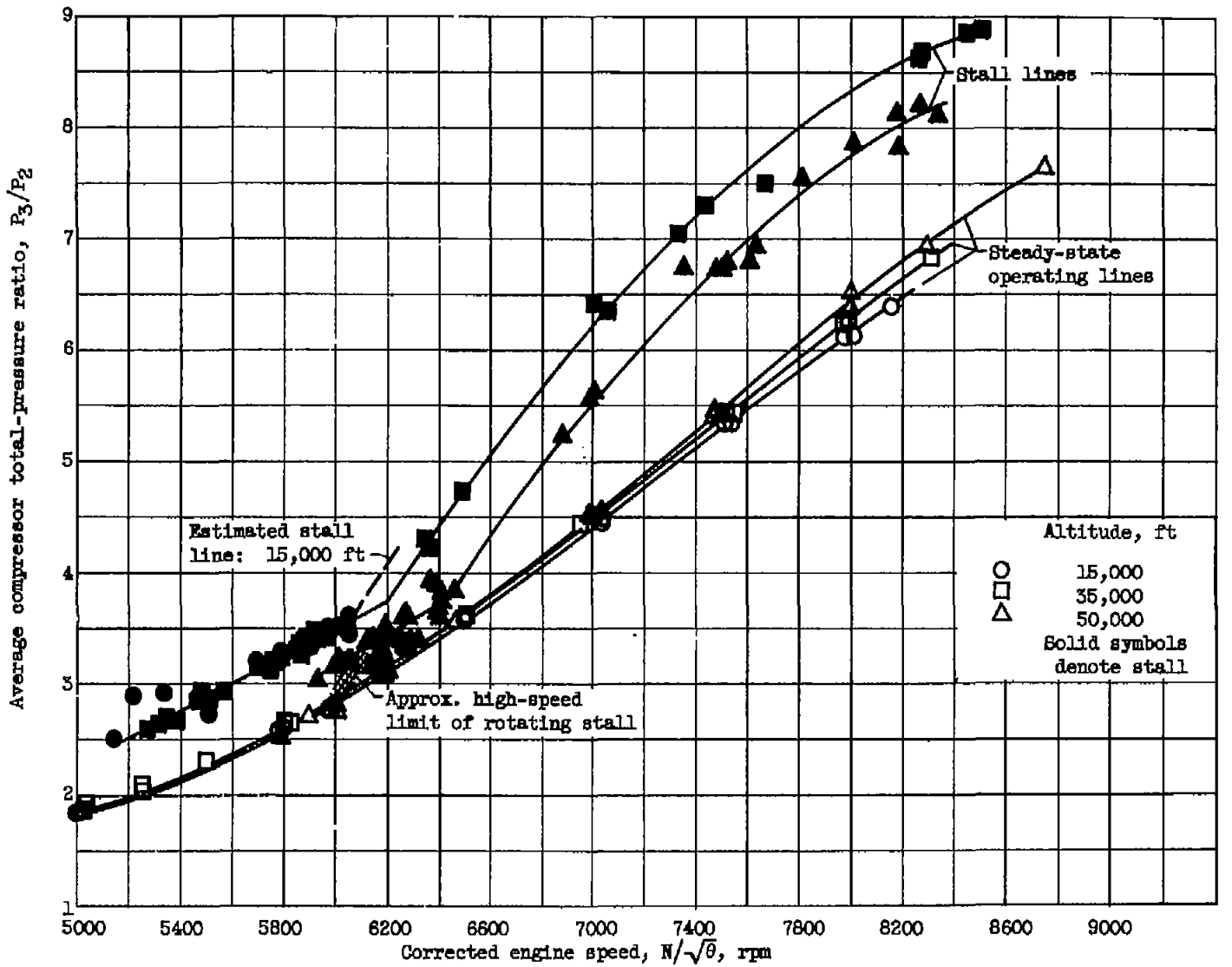

Figure 8. - Effect of altitude on compressor-stall pressure ratio with uniform inlet flow. Flight Mach number, 0.8.

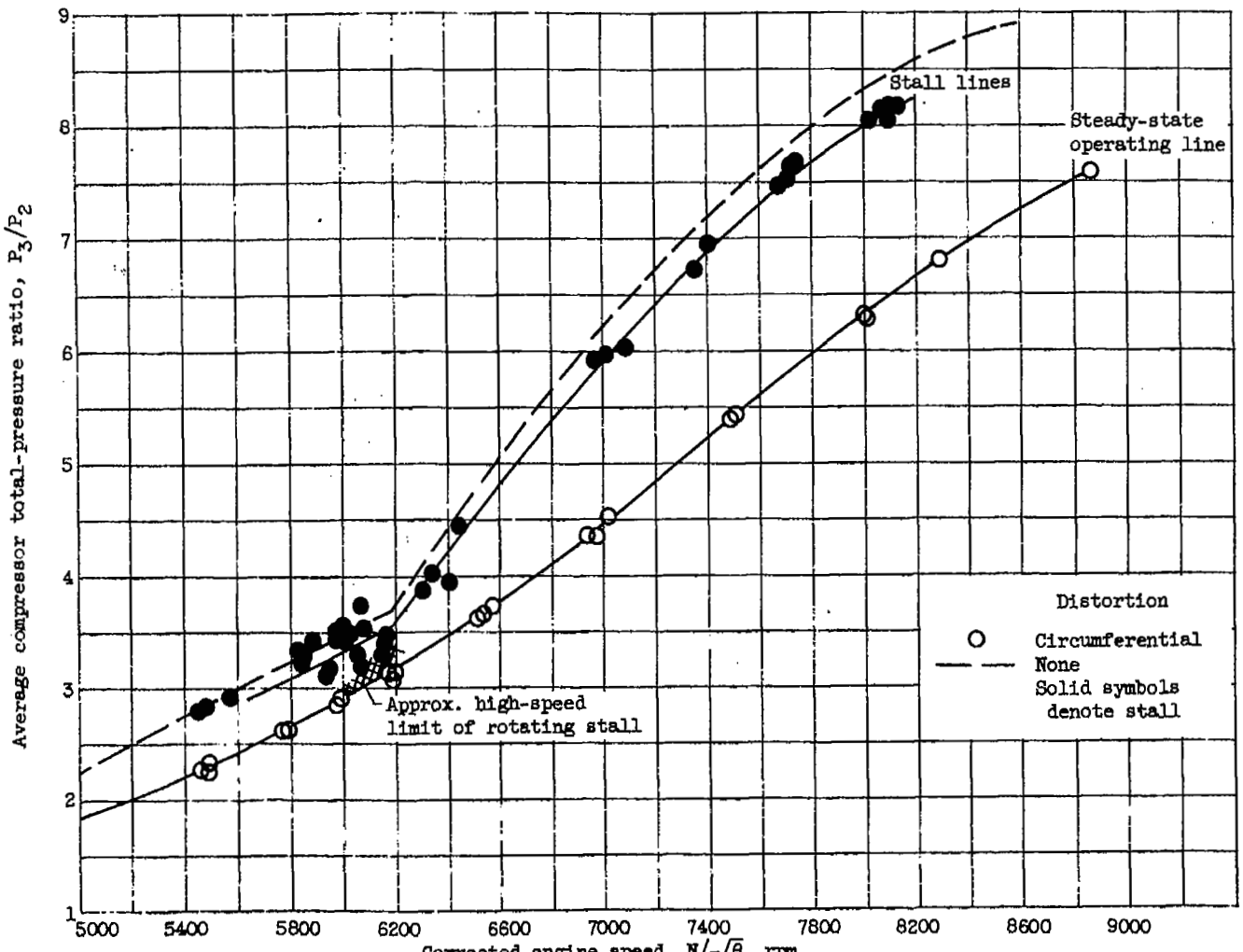

(a) Average compressor total-pressure ratio.

Figure 9. - Effect of circumferential distortion on compressor-stall pressure ratio. Altitude, 35,000 feet; flight Mach number, 0.8.

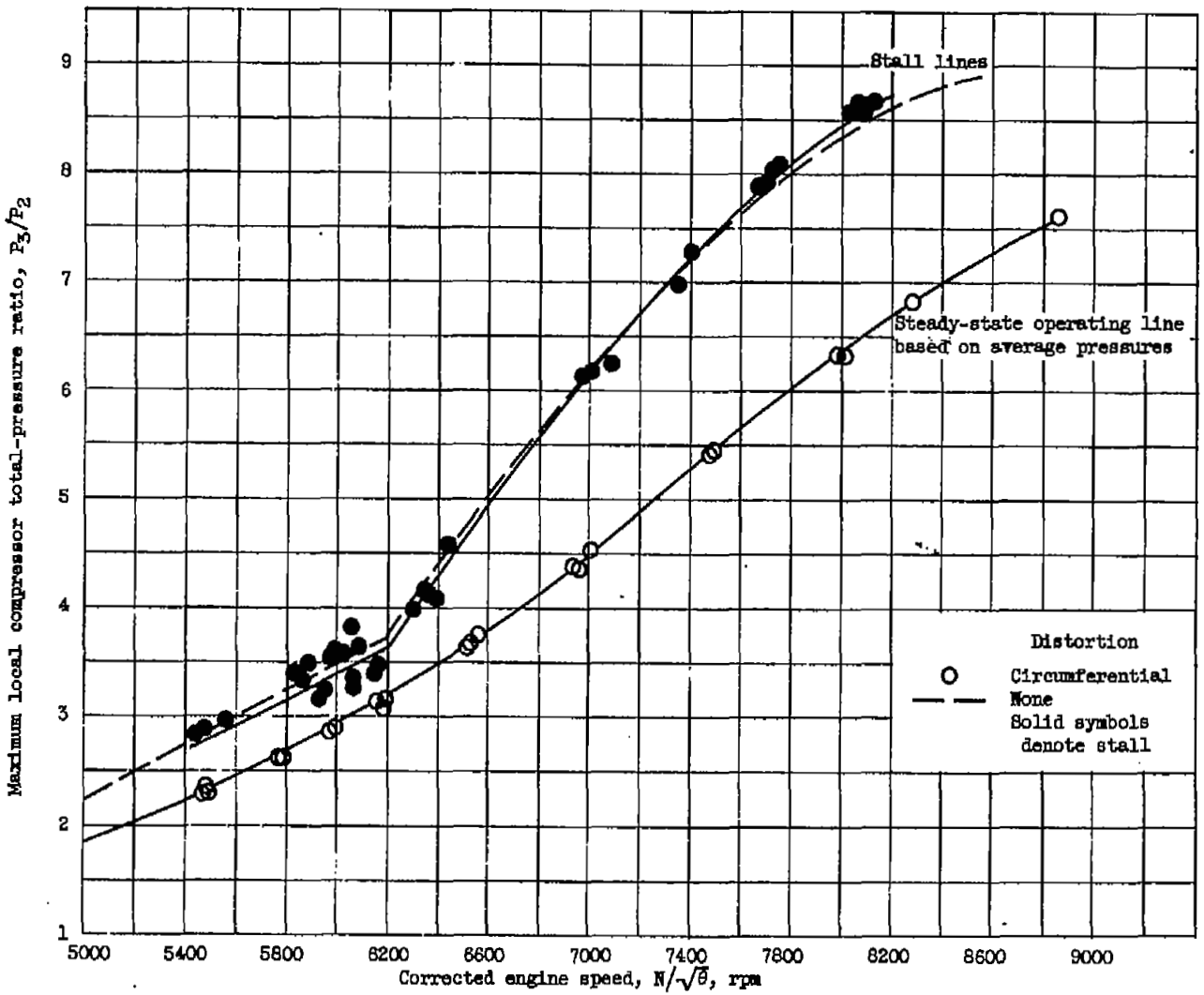

(b) Maximum local compressor total-pressure ratio.

Figure 9. - Concluded. Effect of circumferential distortion on compressor-stall pressure ratio. Altitude, 35,000 feet; flight Mach number, 0.8.

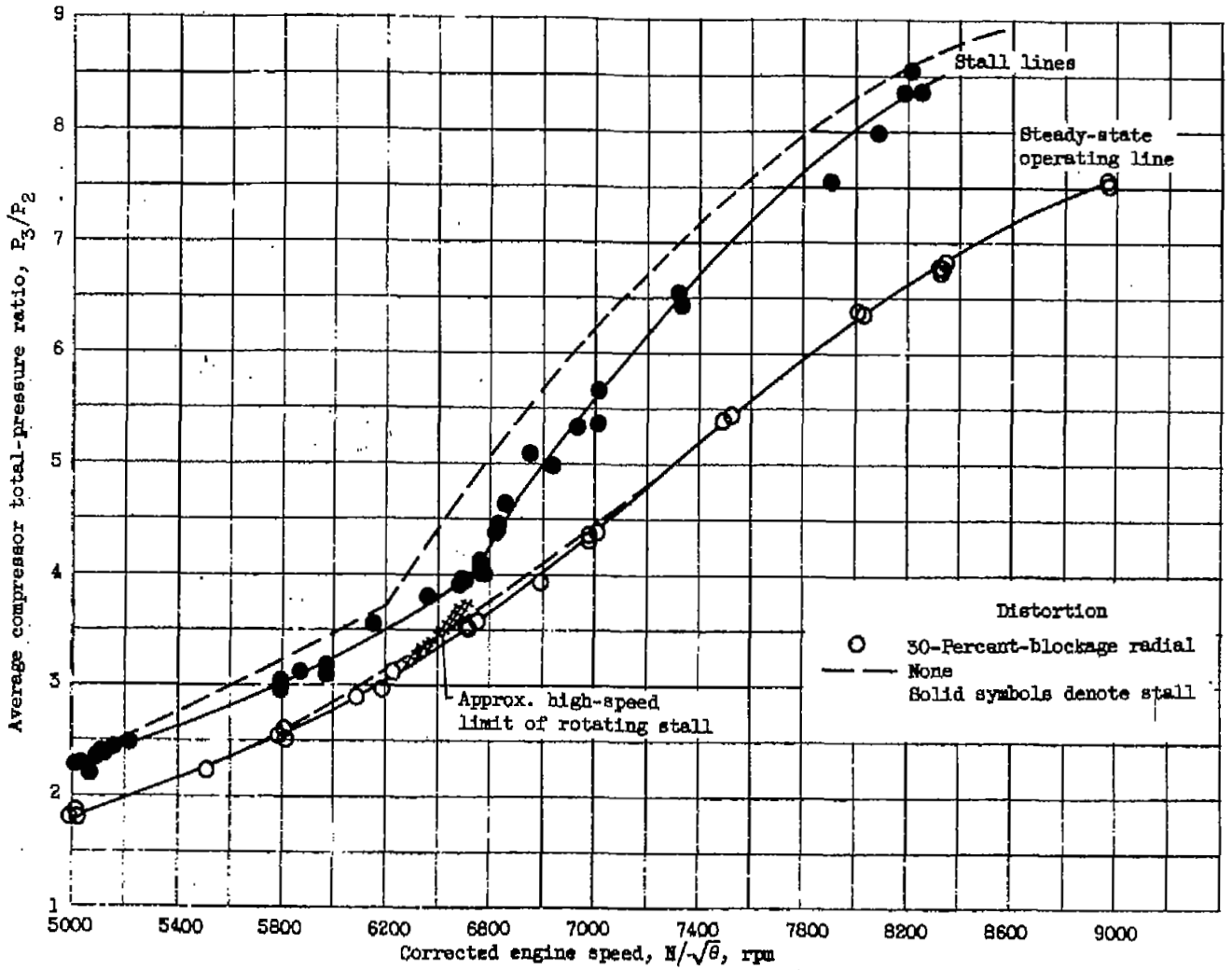

(a) 30-Percent-blockage radial distortion; altitude, 35,000 feet.

Figure 10. - Effect of radial distortion on compressor-stall pressure ratio. Flight Mach number, 0.8.

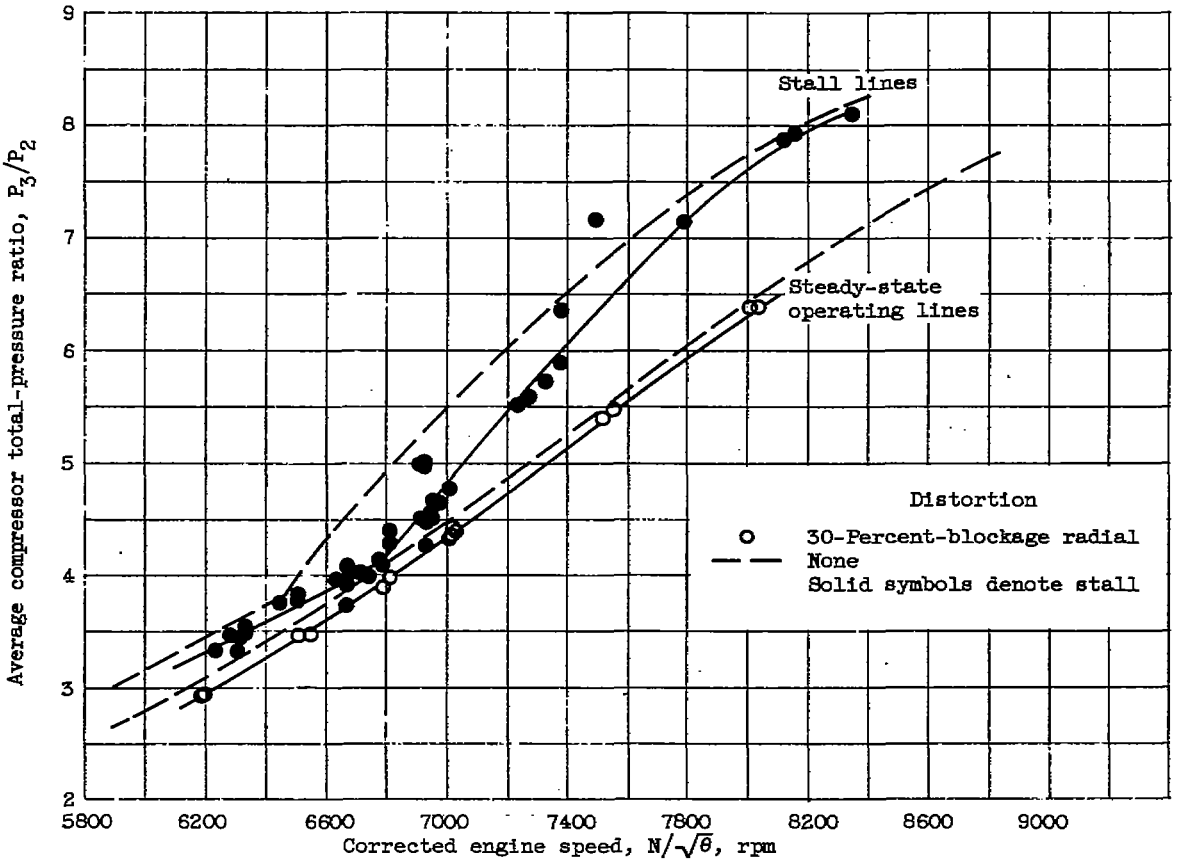

(b) 30-Percent-blockage radial distortion; altitude, 50,000 feet.

Figure 10. - Continued. Effect of radial distortion on compressor-stall pressure ratio. Flight Mach number, 0.8.

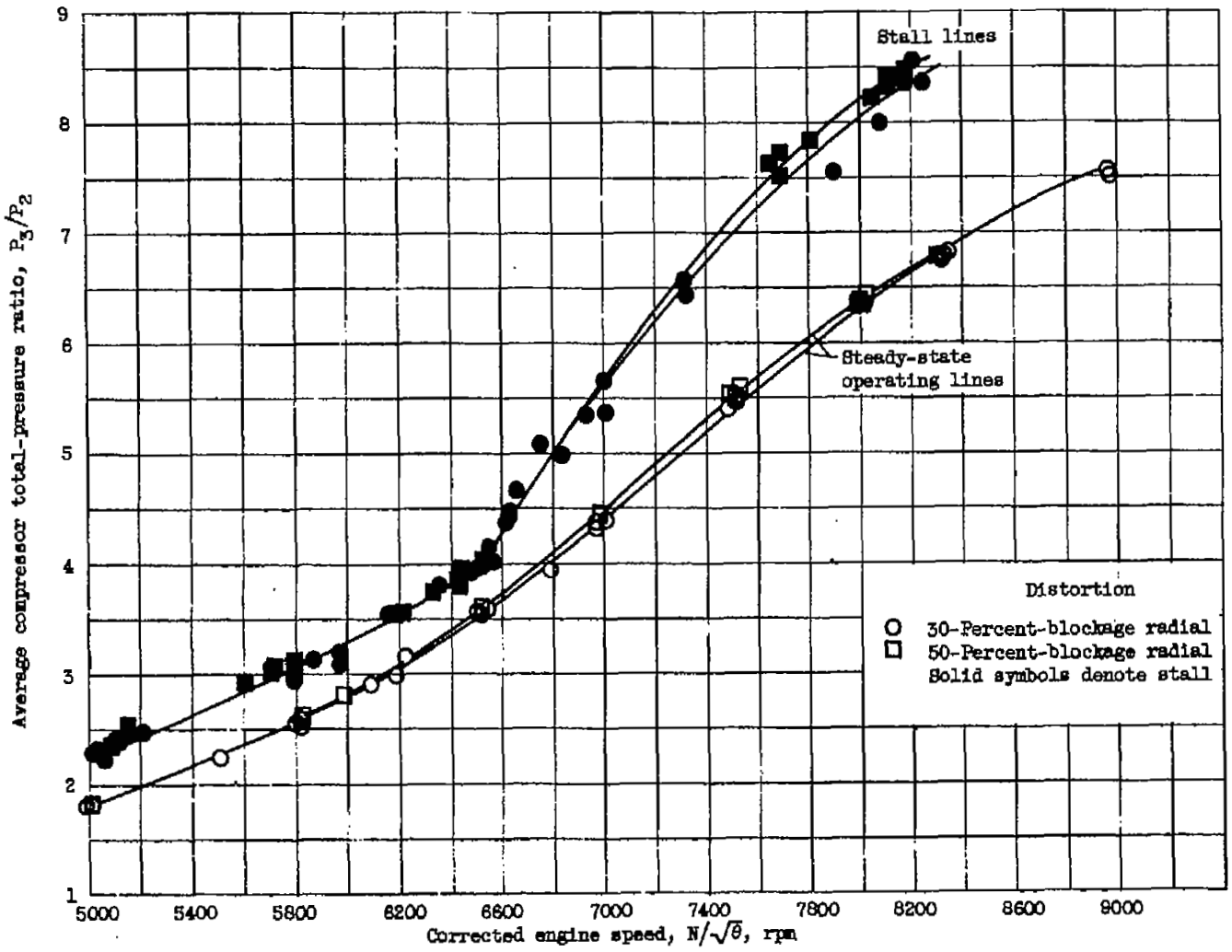

(c) 50-Percent-blockage radial distortion; altitude, 35,000 feet.

Figure 10. - Concluded. Effect of radial distortion on compressor-stall pressure ratio. Flight Mach number, 0.8.

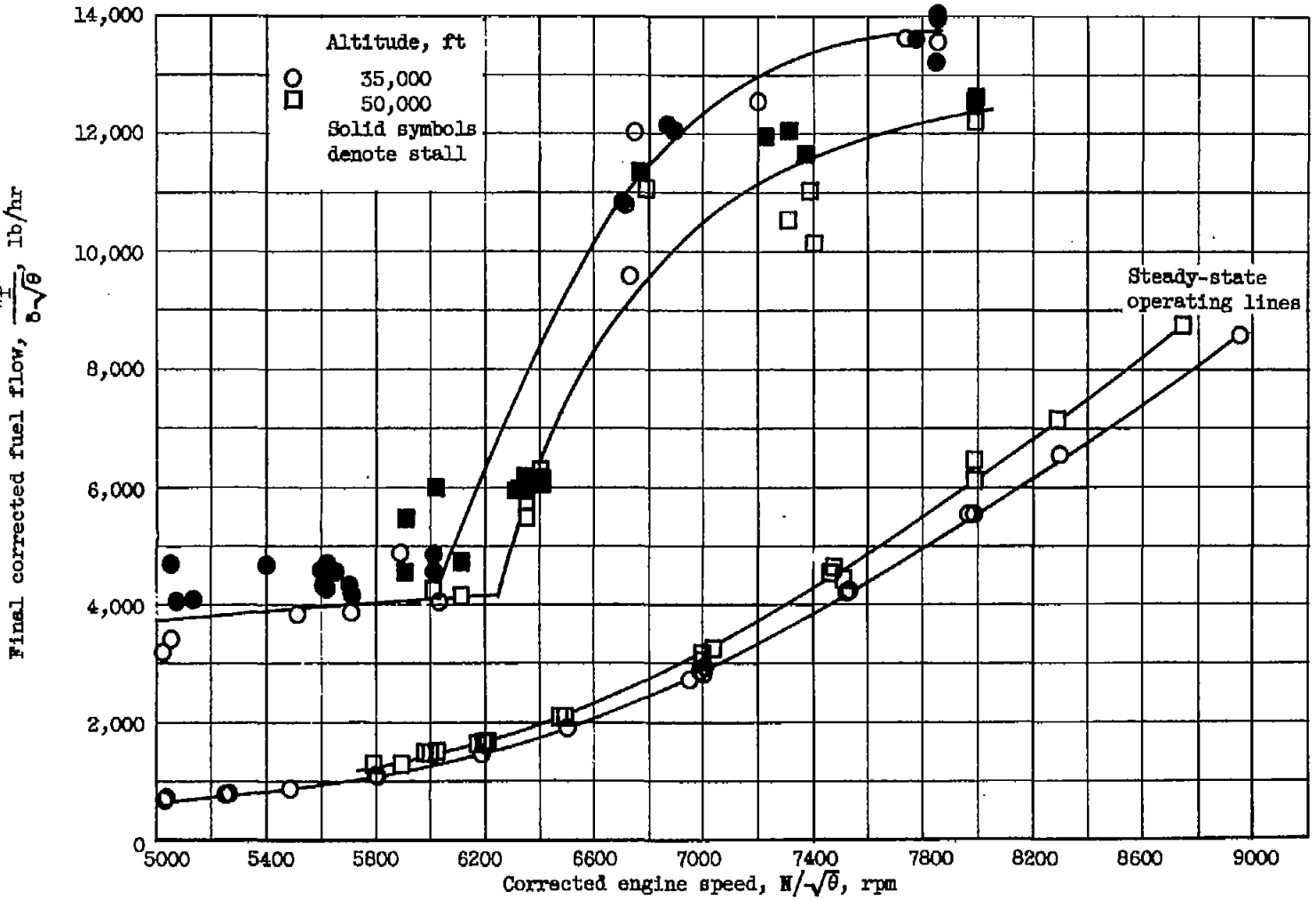

Figure 11. - Effect of altitude on fuel step for stall. Uniform inlet flow; flight Mach number, 0.8.

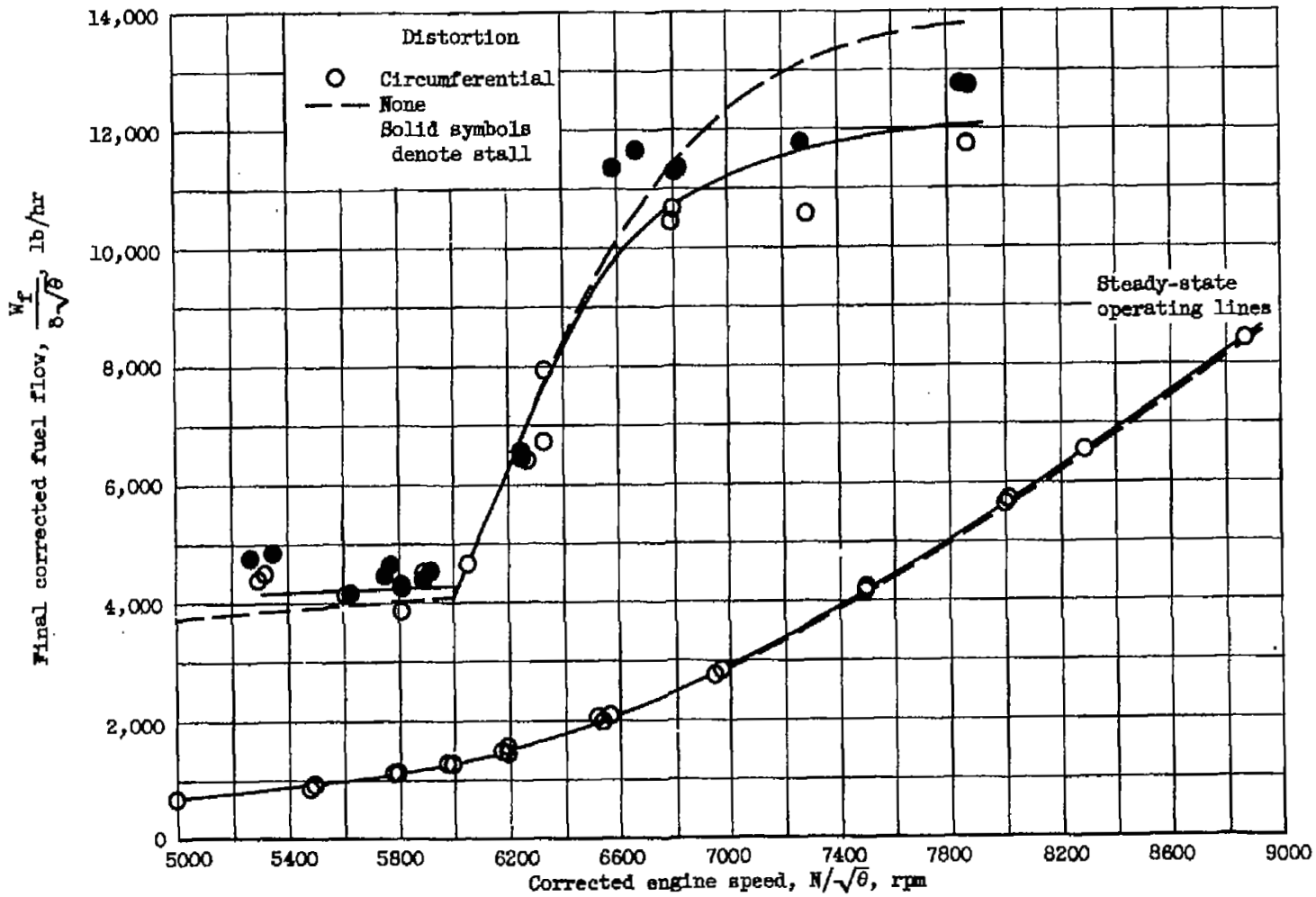

(a) Circumferential distortion.

Figure 12. - Effect of inlet flow distortion on fuel step for stall. Altitude, 35,000 feet; flight Mach number, 0.8.

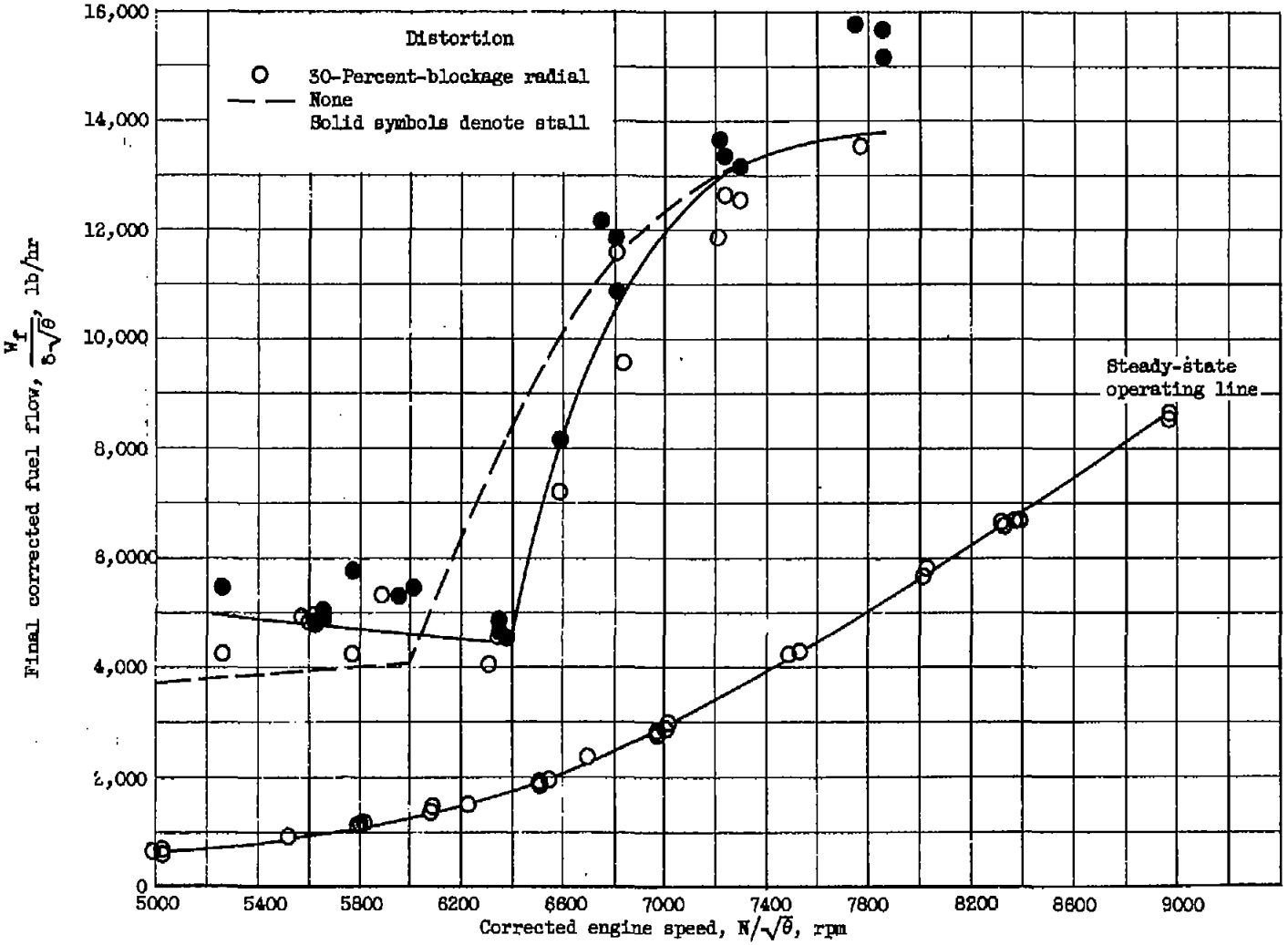

(b) 30-Percent-blockage radial distortion.

Figure 12. - Concluded. Effect of inlet flow distortion on fuel step for stall. Altitude, 35,000 feet; flight Mach number, 0.8.

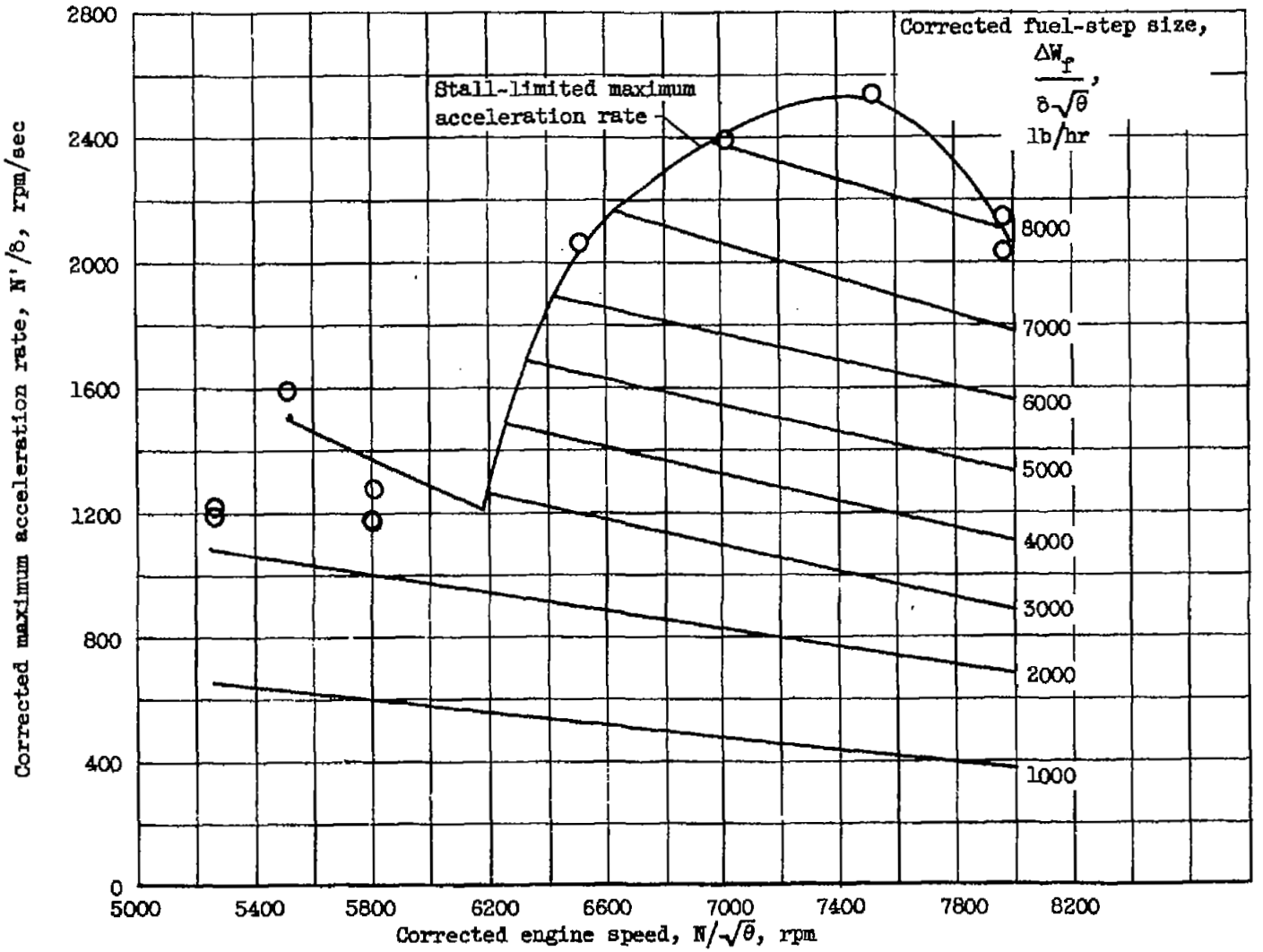

Figure 13. - Maximum acceleration rate following fuel steps. Uniform inlet flow; altitude, 35,000 feet; flight Mach number, 0.8.

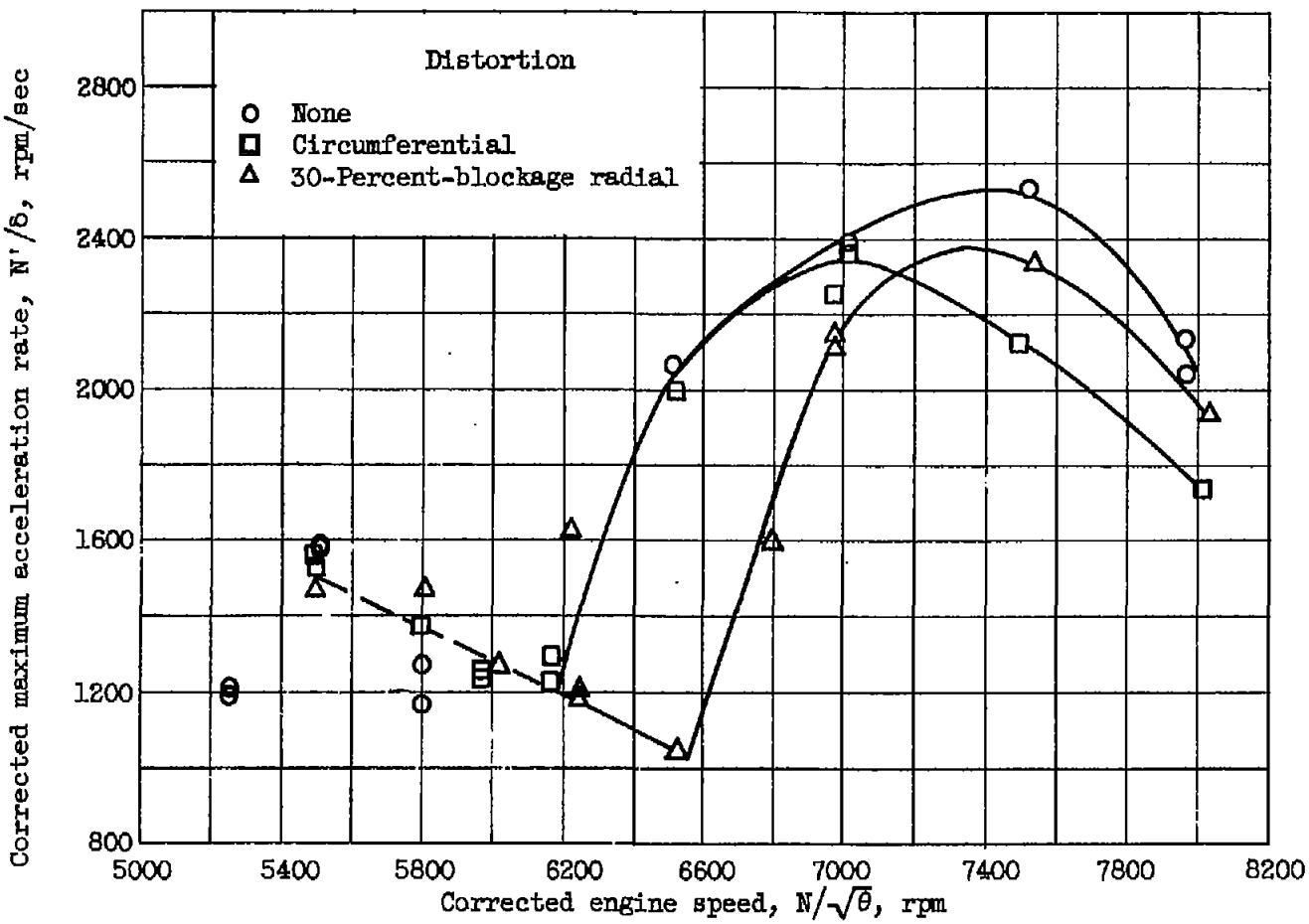

Figure 14. - Effect of inlet flow distortion on stall-limited maximum acceleration rate of engine. Altitude, 35,000 feet; flight Mach number, 0.8.

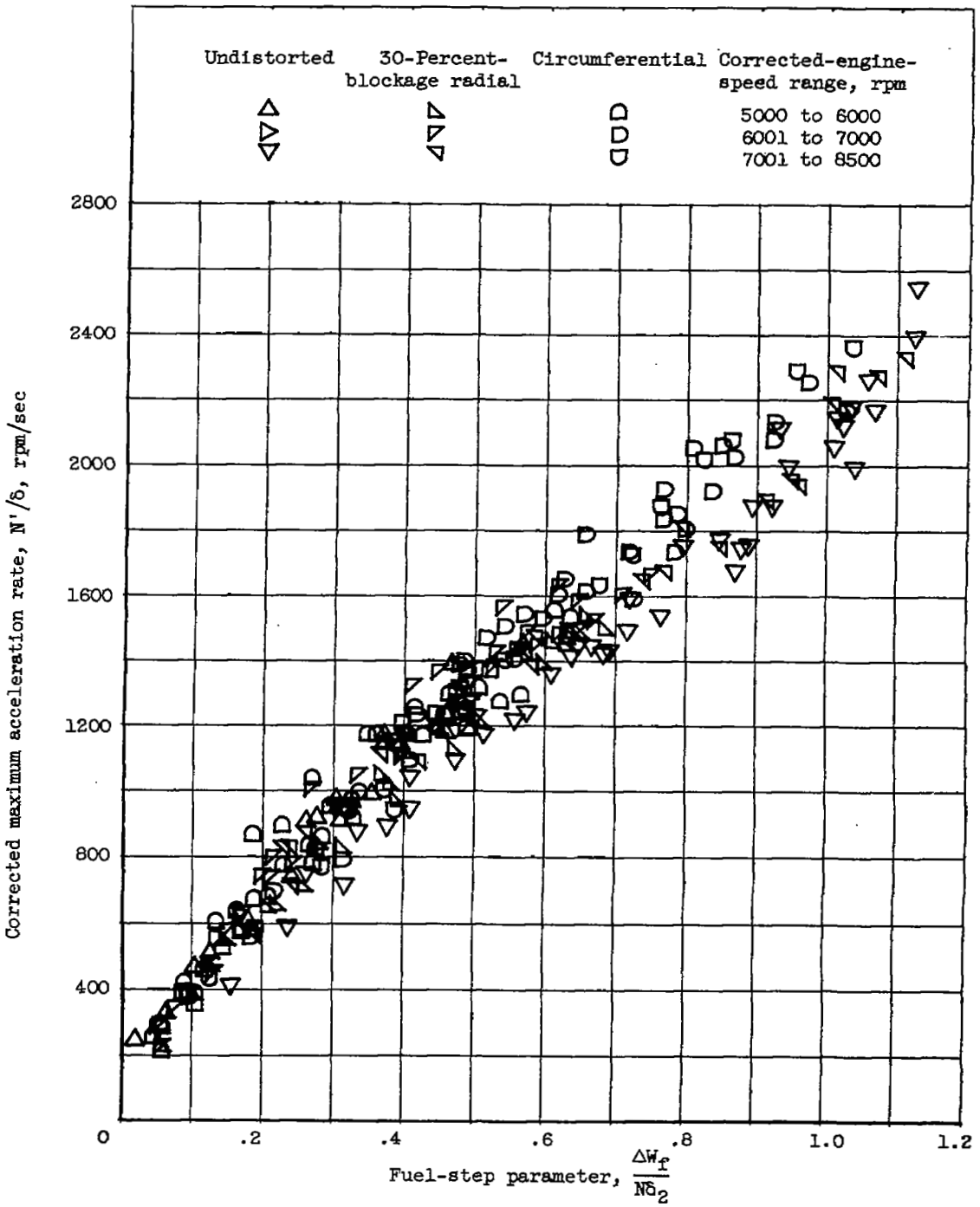

Figure 15. - Effect of inlet flow distortion on maximum acceleration rate of engine following any stall-free fuel step. Altitude, 35,000 feet; flight Mach number, 0.8.